Nuclear forensics: searching for nuclear device debris in trinitite-hosted inclusions

Jeremy J. Bellucci · Antonio Simonetti

Abstract This study documents the 3D morphology of trinitite-hosted metallic inclusions and the first observations of alloys consisting primarily of Pb, Ta, Ga, and W. Scanning electron and backscatter electron imaging, as well as energy dispersive X-ray spectra chemical composition data are reported for heavy metal inclusions in 14 different samples of trinitite. Inclusions consisting of Fe–Ti–Si are the most abundant and presumably derived predominantly from the explosion tower. Grains of Cu, Pb, Ta + Ga + W were also observed and are likely derivatives of the trinitite device wiring, tamper, and tamper and core, respectively. Additionally, a Ba-rich grain and multiple zircons ($ZrSiO_4$) were observed in a large majority of samples. The spherical morphology and the ubiquitous positioning of the heavy metal inclusions on the crater walls of the glassy trinitite surfaces indicate a two-step formation. Stage one involves formation of the glassy trinitite, while the second stage involved the precipitation of the inclusions that were incorporated onto the surface of the trinitite. Furthermore, the precarious positioning of these inclusions further emphasizes the need for analysis using non-destructive techniques prior to methods employing a bulk sample digestion approach.

Keywords Nuclear forensics · Trinitite · In situ analyzes · Scanning electron microscopy

J. J. Bellucci (✉) · A. Simonetti
Department of Civil Engineering and Geological Sciences,
Notre Dame University, Notre Dame, IN 46556, USA
e-mail: jeremy.bellucci@gmail.com

Introduction

Nuclear proliferation is, arguably, one of the greatest threats to modern civilization. The most effective measure at reducing the risk of a nuclear incident is by decreasing the amount of active warheads. The new Strategic Arms Reduction Treaty (START) treaty, signed in February 2011, is charged with both monitoring and disarming the United States and Russian Federation nuclear arsenals. Seven countries, and a looming 8th, have nuclear capability and have not participated in anti-nuclear proliferation talks. It is unlikely that a traditional nation or state would detonate an atomic weapon in an act of war; more likely, any devices detonated will be from a non-traditional or transitory group that has procured a device or fissile material through the black market, or a government that sponsors terrorism. Therefore, understanding how to reconstruct a nuclear weapon from its post-detonation products, and determine provenance of the materials will allow for accurate and rapid attribution. The main goal of the burgeoning field of "nuclear forensics", which investigates post-detonation materials from the impact site, is to resolve the source of materials used in the nuclear device and to identify these from the surrounding (natural) environment.

The Trinity test started the "atomic age" in the early morning hours of 16 July 1945 at the White Sands Proving grounds with the detonation of the first atomic bomb. The detonated device, "gadget" was a plutonium-based implosion device similar to the "Fat Man" device used to destroy Nagasaki, Japan on 9 August 1945. The "gadget" specifications are as follows: a Pu–Ga alloy core, $^{240}Pu/^{239}Pu = 0.0128$–0.016 mol/mole [1, 2]; a tamper of natural U composition; organic-based explosives, and aluminum shells. The bomb was hoisted to an elevation of 30 ft using a steel bomb tower before detonation. Upon

detonation, a 21 kiloton explosion fueled a fireball with a temperature of 8,430 K that reached an elevation of 15.2–21.3 km [3]. The fireball entrained pieces of the device and existing geology and structures, creating a green-glassy material named trinitite (after the name of the first test, "Trinity"). Since trinitite is the post-detonation material, it is naturally the primary target for investigations hoping to apply nuclear forensics to the "gadget" device. Additionally, since the construction and materials used in the "gadget" device are known, examination of trinitite is a good test for any proposed nuclear forensics-based procedures.

Several previous studies have focused on the radiochemistry aspects of trinitite (e.g., [1, 2, 4]). Here, this study focuses specifically on surface morphological features including the presence of inclusions that are imaged with scanning electron microscopy (SEM), backscatter electron (BSE) imaging, and energy dispersive X-ray spectra (EDS) in an attempt to provide insights into: (1) identifying inclusions for forensic applications and thereby recognizing components that will aid in the reconstruction of the device, and (2) morphological features that will aid in identifying the chemical/physical properties of the atomic explosion. In situ techniques, as employed here, are necessary when investigating trinitite because of its well-documented extreme heterogeneity at the micron-scale [1–4].

Trinitite is expected to consist of a mixture of components from the primary, regional geological materials and those from the blast sight/bomb itself. The geology of the White Sands Proving ground is sedimentary in nature with alluvial, aeolian, and volcanic provenances. The primary rock type in the region is arkosic sandstone, and contains minor amounts of feldspar (microcline and albite), carbonates, sulfates, chlorites, clay, and mafic minerals (i.e., hornblende, olivine, magnetite, ilmenite, augite [1, 3, 5–7]). Understanding the primary geology is important in relation to distinguishing bomb components, which is the ultimate goal of a nuclear forensics study. On the basis of their chemical compositions, the most discernable contrasts between the bomb-related materials and surrounding geology are metals (Fe, Pb) and radionuclides (Pu, U, and related activation/fission products). Metals, such as Fe is typically present at low abundances in arkosic sandstone (<1wt% FeO_{total}, e.g., [9]) and therefore, our investigation has targeted primarily inclusions with a high mean atomic weight (i.e., >50/amu) using BSE analysis. Subsequently, SEM imagery will serve to illustrate the morphology of the different inclusions. Post-identification, "semi-quantitative" EDS analyzes were conducted in order to determine the chemical composition of all of the inclusions.

Trinitite samples spanning 14 different groups (Supplementary materials) were purchased from Mineralogical Research Corporation (http://www.minresco.com). The relative spatial distribution of these samples is unknown. Using the compositional data and morphology of the trinitite-hosted inclusions, forensic, and explosion mechanism hypotheses are proposed.

Methods

All analyzes were performed at the University of Notre Dame Integrated Imaging Facility using the Leo SEM. Samples were prepared for the SEM by coating them with ~4–5 nm layer of Ir. Images and EDS spectra were captured using an accelerating voltage of 20 kV. Chemical compositions were determined using EDS, which yields an internal precision on major elements (concentrations of >1wt%) of ±10% (2σ level). While this technique does not yield highly precise analyzes, there are several advantages when compared to more invasive techniques: (1) it is completely non-destructive and (2) minimal sample preparation, which allows for the characterization of a significant number of samples in a relatively short period of time. Due to the non-destructive nature of this sampling technique, viewing of the pristine surface morphology of these samples and inclusions was possible. Moreover, this allowed for the preservation of micron-sized inclusions that could be lost during preparation of standard petrographic thin sections.

Results

Trinitite samples investigated here that contain metal inclusions are listed in Table 1. The EDS spectrum for each inclusion is included in the Supplementary materials. Additionally, chemical compositions of trinitite glass obtained here are compared to those reported in the literature (Supplementary materials and Supplementary Fig. S1).

Iron–silica–titanium

The most common type of metal inclusions found were Fe–Si alloys with flat topography (Table 1; Fig. 1). Most of these inclusions have border regions with less Fe than the center indicating a mixture with the surrounding Si-rich matrix (Fig. 1a, b). Similarly, the amorphous/bleb/dumbbell morphology of these inclusions indicates a melt/liquid origin (e.g., [8]). This hypothesis is substantiated by the presence of inclusions with dendrite iron crystallization patterns (Fig. 1c, d) which has also been observed by Fahey et al. [1]. The presence of dendrites suggests the co-existence of immiscible Fe- and Si-rich liquids, which upon cooling produced this texture. These inclusions are

Table 1 Trinitite samples and inclusions

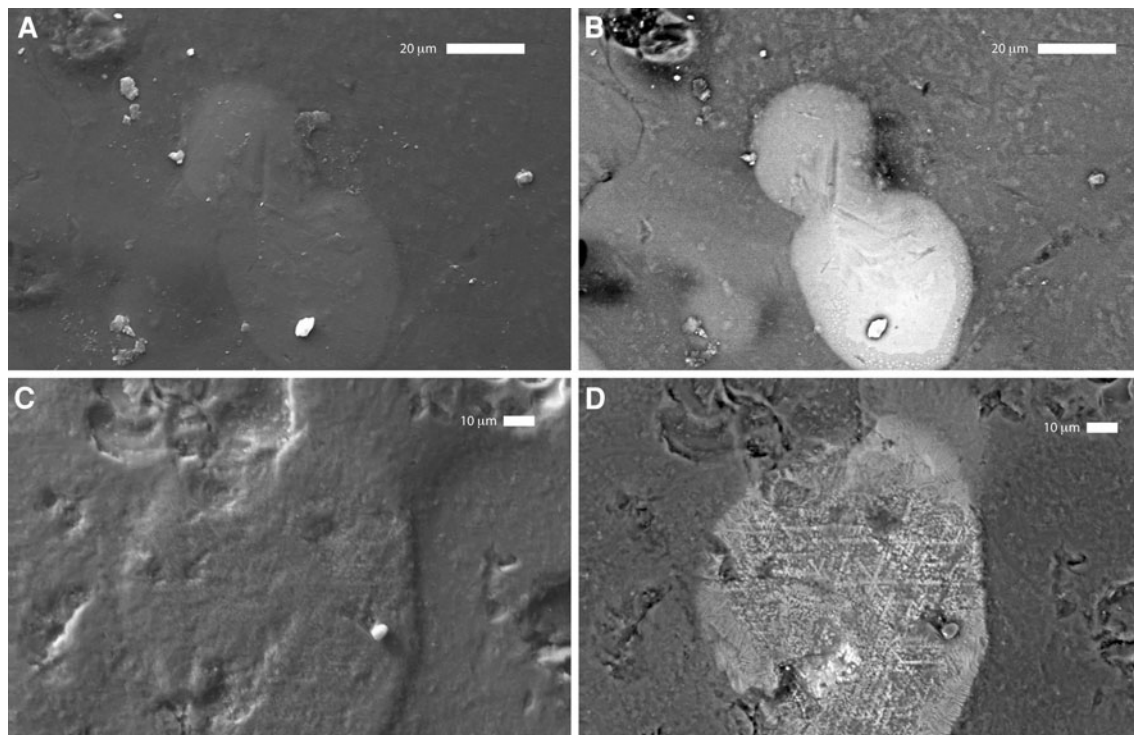| Sample	FeO	Fe–Si	Fe–Ti	Ti	Pb	W	Zircon	Cu	Ba
1	×	×							
2		×			×	×	×		
3		×	×	×			×		×
4A		×	×					×	
4B	×	×	×					×	
4C		×	×				×		
4D									
4E		×							
4F	×	×							
5A		×	×				×		
5B		×					×		
5D		×	×				×		
5E	×	x	×				×		
5F	×	×					×		

Fig. 1 SEM (**a**) and BSE (**b**) images of a Fe–Si inclusion, SEM (**c**) and BSE (**d**) image of a Fe–Si inclusion with Fe crystallization inside the grain, the dendritic morphology is readily apparent in 1D

enveloped by the trinitite glass, and therefore had to have formed contemporaneously.

Another type of Fe inclusion consists mainly of Fe and Ti that contains little Si (<5wt%) and has a significant topography (Fig. 2a). The inclusion displayed in Fig. 2a, b also exhibits exsolution features in BSE. Based on their lower "topography" (i.e., relative height above the sample surface) compared to the Fe–Si–inclusions

(Fig. 1), the Fe–Ti inclusions do not seem to have cooled as liquids (or molten material) within the trinitite matrix. One trinitite sample contained a grain of almost pure Ti (Fig. 2c, d). Titanium-rich lathes were also observed by Fahey et al. [1], but these were enclosed within a Si-dominated matrix. The Ti–rich grain shown in Fig. 2 is located on a crater wall, not bound or engulfed by the trinitite matrix.
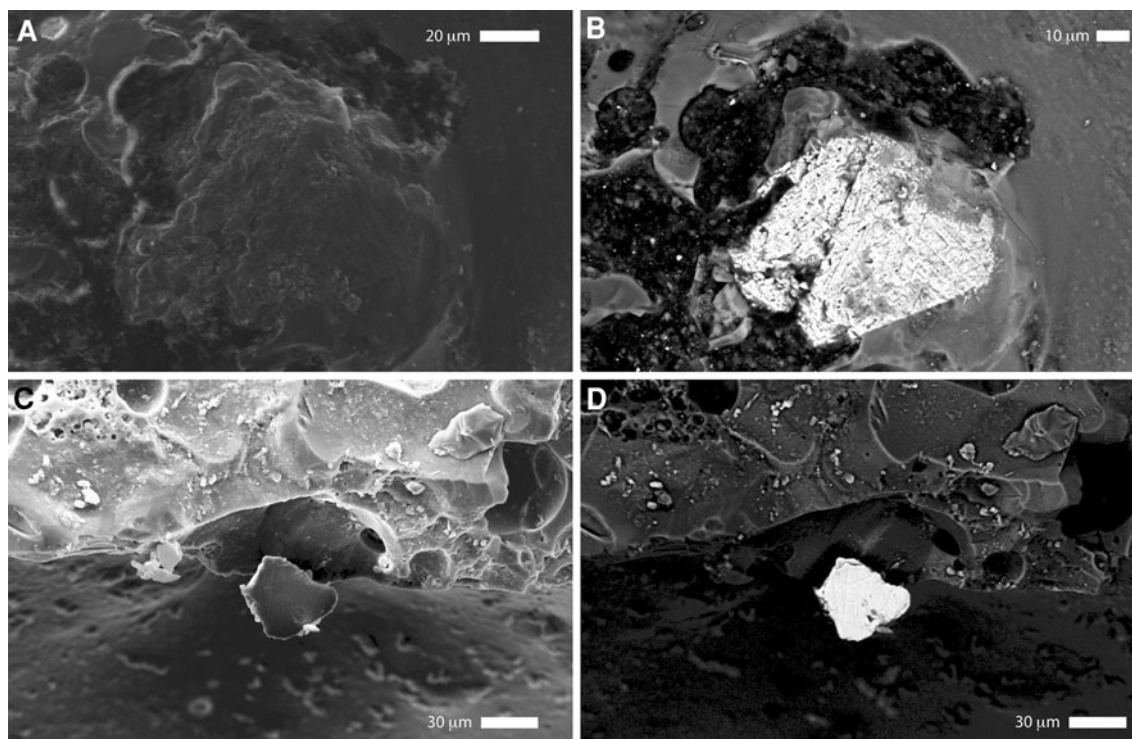
Fig. 2 SEM (a) and BSE (b) images of a Fe–Ti inclusion. Note the exsolution features in 2B. SEM (c) and BSE (d) image of a Ti inclusion

Copper

Copper-bearing inclusions have been observed in trinitite [3] and are characterized by a distinct red color. In the "red variety" of trinitite samples, the inclusions consist mainly of Cu–S (Fig. 3). Their morphology is roughly spherical with globular features on the surface. They have a small diameter ∼10 μm and appear to be located on the walls of the cratered trinitite surface, which is analogous to the Ti inclusions (Fig. 2). Moreover, their spherical nature is similar to the metal "chondrules" observed by Eby et al. [3] in the "red variety" of trinitite.

Lead

Minor Pb-bearing inclusions have been observed in metal chondrules of trinitite [3]; however, the occurrence of a major Pb-bearing phase has not been previously reported in trinitite. Two examples of almost pure PbO spherules are located on the crater walls of trinitite sample 2 (Fig. 4). The Pb particles define a spherical shape with a diameter of ∼20 μm, but have tendrils off-shooting from the main body of the particle (Fig. 4). Fahey et al. [1] demonstrated that the Pb isotopic composition of Pu-enriched regions of trinitite is "radiogenic" (i.e., high $^{207}Pb/^{206}Pb$ value) and distinct compared to that for the natural or "common Pb" derived from the desert sand; this "radiogenic" Pb was

attributed to originating from the 235-enriched uranium used in the tamper material for the device [1]. Thus, determining the Pb isotopic composition of Pb particles/inclusions may prove as an effective forensics/fingerprinting tool for nuclear devices in post-detonation materials (e.g., [10–12]).

Tungsten

A single grain of a W–Ga–Ta alloy was found on the crater wall of one sample (Fig. 5a, b). The grain is ∼30 μm long and ∼10 μm wide. To our knowledge, no W, Ga, or Ta grains, let alone alloyed, have ever been previously observed in trinitite.

Miscellaneous

Inclusions of zircon ($ZrSiO_4$), located within the trinitite matrix, and a Ba-rich phase were also found. Fahey et al. [1] also described both Ba-rich regions and Zr-rich inclusions in trinitite; the latter is not surprising given that detrital $ZrSiO_4$ (erosional products from surrounding rocks) are a common occurrence in sandstone. Figure 5c, d shows a small grain (∼10 μm × ∼10 μm) consisting mainly of Ba and S residing on the wall of a trinitite crater. The high amount of sulfur suggests that this inclusion may represent a grain of barite ($BaSO_4$) contained within the
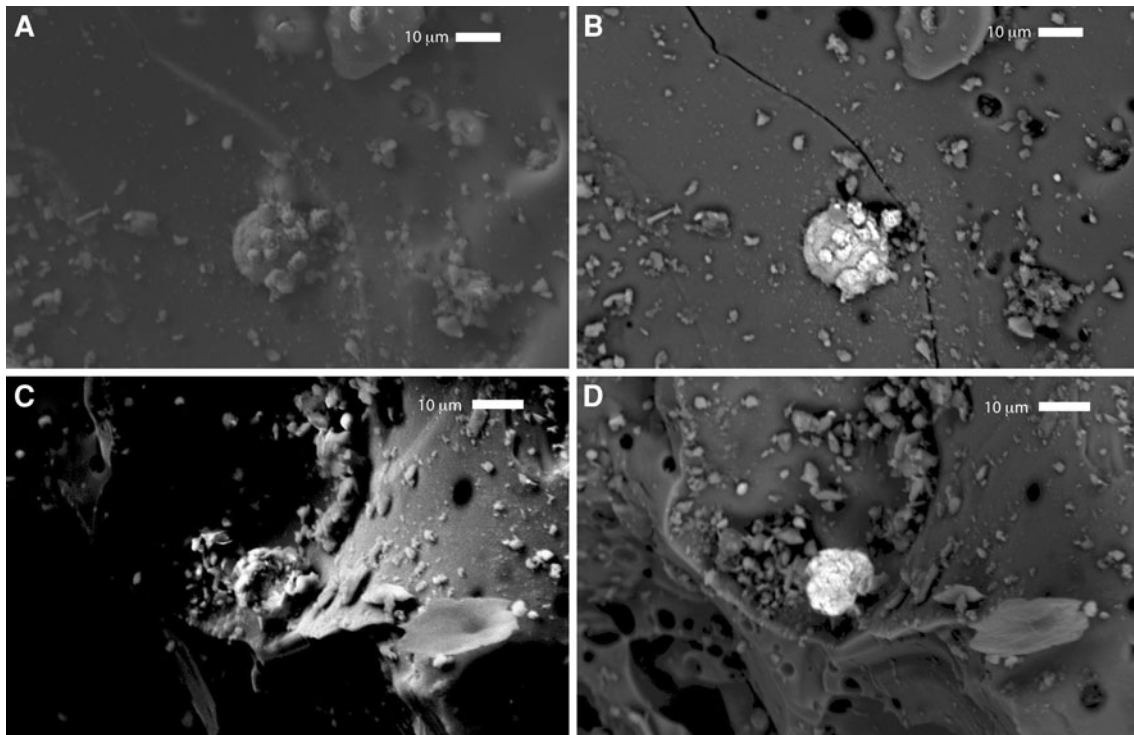
Fig. 3 SEM (**a**, **c**) and BSE (**b**, **d**) of Cu inclusions
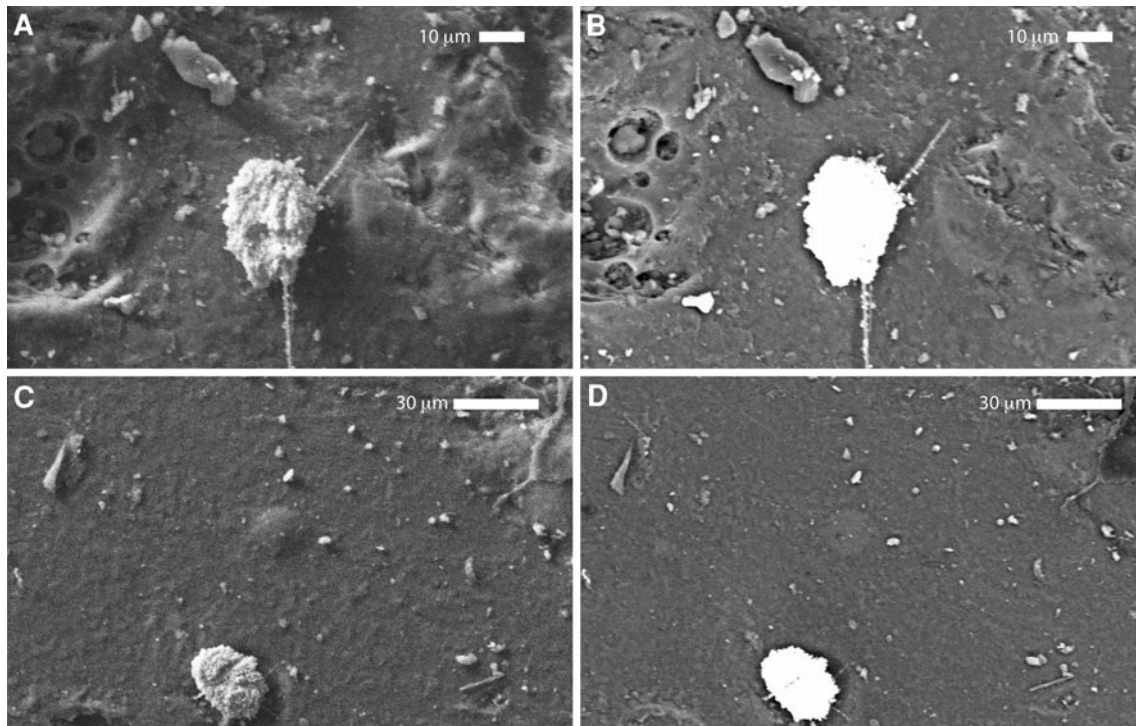

Fig. 4 SEM (**a**, **c**) and BSE (**b**, **d**) of Pb inclusions

precursor desert sand since it contains abundant salt and sulfate deposits. Barium and Ba-bearing phases are of specific interest since they could incorporate [133]Ba, which can be used in forensic investigations because $Ba(NO_3)_2$ was used in the production of the explosives employed within the "gadget" device [13].
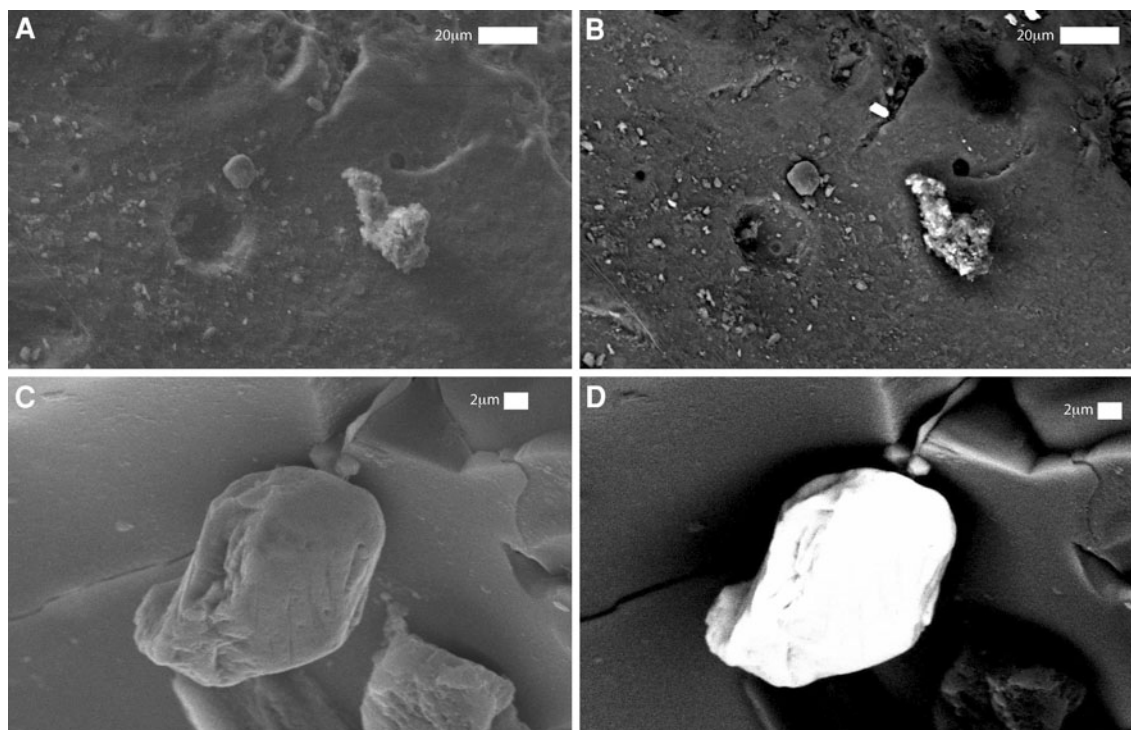
Fig. 5 SEM (**a**) and BSE (**b**) images of a W–Ta–Ga inclusion, SEM (**c**) and BSE (**d**) image of a Ba inclusion

Discussion

Forensic implications

Following the Trinity detonation, Hans Bethe (a Nobel Laureate physicist) noted that, "All the structures in the immediate area were essentially destroyed and droplets of molten metal were dispersed to the north of ground zero". This statement, combined with the fact that the arkosic sandstone (the natural geologic background material) does not inherently contain significant components of heavy metal, leads to a fair assumption that the majority of metal grains described above were derived from the device and/or materials/structures surrounding the explosion. Hence, the following hypotheses are proposed for the origin of the inclusions/grains documented in this study. The inclusions that consist of Fe–Ti–O, which have been noted in previous studies, most likely derive from the blast tower proper. The spherical Cu grains most probably originate from the wiring used in the device. Copper is not present in significant amounts in the region (ppm level; e.g., [14]), and Cu was solely used in the wiring during construction of the device (e.g., [3]). The inclusions of Pb were an unexpected find, as inclusions of this type have never been previously described. Lead is a heavy metal that is a good neutron reflector, which could have been incorporated into the natural U tamper during the refinement process. Therefore, the majority of the Pb inclusions are most likely derived from the tamper in the "gadget" device. Similarly, both Ta and W are good neutron reflectors, but their use in the construction of the Trinity device has not been observed nor documented. The presence of Ga in this inclusion corroborates its derivation from the device, as Ga is commonly alloyed with Pu in the enrichment process. It is quite possible that during detonation, the tamper (W and Ta) must have alloyed with the Ga from the core to produce this grain. The origin of the Ba-bearing grain cannot be discerned from the evidences reported here since, as explained previously, it is possibly derived from the local geology.

Explosion processes

Belloni et al. [4] proposed a two-stage formation process for trinitite. Based on the textures, morphologies, and positioning of the inclusions investigated here, their formation is consistent with a two-stage process. The first involves the incorporation of a certain volume of the arkosic sandstone into the fireball, and is followed by the "raining down" of device, geological, and explosion site materials from the cloud, which fuses into trinitite. However, their precipitation from the cloud must have occurred at some point later in time so as to permit cooling and solidification of the trinitite matrix prior to the incorporation of solid-type inclusions (e.g., Fe–Ti; Fig. 2). A sustained precipitation of debris would be required in order to

have the glass fuse and subsequently add debris. Additionally, the "strands" radiating from the Pb inclusion (Fig. 4a, b) resemble Pele's hair, a rock texture that is formed when lava is ejected into the atmosphere and is wind-spun into spindles (e.g., [15]).

Conclusions

Morphological, spatial, and compositional data for new types of metal inclusions investigated here are likely to have been derived from the "gadget" device and materials from the explosion site. Utilizing non-destructive SEM-based methods, insights have been gained about the metal inclusions and the formation of trinitite. There are two types of Fe–Ti–Si inclusions based on their level of "topography" or height above the trinitite surface; those lacking topography or height are dumbbell-shaped and likely formed and precipitated within the cloud along with the glassy trinitite. The Fe–Ti inclusions with topography likely followed and were adhered to the surface as solid pieces. The Cu inclusions likely derive from the device's wiring. The Pb inclusions most probably originate from the tamper. The W, Ta, and Ga alloy is a result of fusion between the core and the tamper. The random locations of the Cu, Pb, Ti, and W + Ta + Ga inclusions on the crater walls suggest a two-stage formation: the first encompassed formation of the trinitite glass, whereas the second involved precipitation of metals and inclusions. The positioning of the inclusions on the crater walls emphasizes the need for non-destructive and micron- (sub-micron-) scale characterization of trinitite, at the very least, during the initial phases of investigation and prior to bulk dissolution methods. Documentation and detailed examination of inclusions and phases such as those reported here can also provide insights for results obtained from bulk chemical treatment of trinitite.

References

1. Fahey AJ, Zeissler CJ, Newbury DE, Davis J, Lindstrom RM (2010) Post-detonation nuclear debris for attribution. Proc Natl Acad Sci USA 107(47):20207–20212
2. Parekh PP, Semkow TM, Torres MA, Haines DK, Cooper JM, Rosenburg PM, Kitto ME (2006) Radioactivity in trinitite six decades later. J Environ Radioact 85:103–120
3. Eby N, Hermes R, Charnley N, Smoliga JA (2010) Trinitite-the atomic rock. Geol Today 26(5):180–185
4. Belloni F, Himbert J, Marzocchi O, Romanello V (2011) Investigating incorporation and distribution of radionuclides in trinitite. J Environ Radioact 102:852–862
5. Love DW, Allen BD, Myers RG (2008) Gypsum crystal morphologies and diverse accumulations of gypsum and other evaporates in the Tularosa basin. N M Geol 30:120–121
6. Staritzky E (1950) Thermal effects of atomic bomb explosions on soils at Trinity and Eniwetok, Los Alamos Scientific Laboratory, LA-1126, pp 21
7. Ross CS (1948) Optical properties of glass from Alamogordo, New Mexico. Am Miner 33:360–362
8. Glass BP, Senftle FE, Muenow DW, Aggrey KE, Thorpe AN (1987) Atomic bomb glass beads: tektite and microtektite analogs. Second International Conference on Natural Glasses, Prague, pp 361–369
9. Pettijohn FJ (1963) Chapter S: the chemical composition of sandstones—excluding carbonate and volcanic sands. In: Fleischer M (ed) Data of geochemistry, US geological survey professional paper, 440-s, p 19
10. Bock B, McLennan SM, Hanson GN (1998) Geochemistry and provenance of the middle Ordovician Austin Glen member (Normanskill formation) and the Taconian orogeny in New England. Sedimentology 45(4):635–655
11. Brill RH, Wampler JM (1967) Isotope studies of ancient lead. Am J Archaeol 71:63–77
12. Fahey AJ, Ritchie NWM, Newbury DE, Small JA (2010) The use of lead isotopic abundances in trace uranium samples for nuclear forensics analysis. J Radioanal Nucl Chem 284(3):575–581
13. Rhodes R (1986) The making of the atomic bomb, 1st edn. Simon and Schuster, New York, pp 575–577, 657
14. Taylor SR, McLennan SM (1995) The geochemical evolution of the continental crust. Rev Geophys 33:241–265
15. Philpotts AR, Ague JJ (2009) Principles of igneous and metamorphic petrology. Cambridge University Press, Cambridge, p 667